Effects of Coconut Coir Powders on the properties of Natural Rubber Composites

Teerakorn Kongkaew[1],Sureeporn Kumneadklang[1],
Jate Panichpakdee[1] and Siriporn Larpkiattaworn[1,*]

Received May 18, 2020; Revised, June 10, 2020; Accepted June 29 2020

Abstract

In this work, the coconut coir powders (CCP)/natural rubber (NR) composites were successfully prepared. The CCP acts as a reinforcing filler with two different sizes of fine powders (39 um) and coarse powders (101 um). The coconut coir powders added to the natural rubber matrix at the filler content of 25, 50, 75, and 100 phr. The effect of CCP contents on physical and mechanical properties was studied. The result revealed that the increase in CCP content has decreased the tensile strength, elongation at break and toughness of composites but increased the modulus of elasticity. The CCP/NR composite at 25 phr of filler loading shows better mechanical properties. For different sizes of fillers, the F-CCP exhibit the better mechanical properties and hardness compare to C-CCP. These properties of composites indicate that it can develop and possible apply in rubber mats.

Keywords: Coconut coir powders, Natural rubber, Mechanical properties, Composites

Introduction

Polymer composites are a combination of a polymer matrix with fillers. They have been attractively applied in industrial and academic researches due to the control of the material properties. For the past few decades, researchers have shown increasing interest in composite materials for those of biodegradable, eco-friendly, and renewable. Natural rubber (NR) as a green and renewable polymer is used extensively in many applications, including in tires, automotive parts, and rubber floor mats, because of its excellent mechanical and elastic properties. However, fillers are essential to modify the NR properties for the versatile application. The capability of the reinforcing filler depends on various factors such as surface area, the shape of fillers, and particle size. Natural fillers have been in enormous demand as a reinforcing material. These fillers act as good reinforcing agents with several specific properties such as high toughness, low cost, lightweight, good specific strength properties, and modulus, and complete burning without residue on the combustion (Ismail et al., 2002; Luz et al., 2007; Panthapulakkal et al., 2006). The natural fibers act as reinforcing natural fillers with biodegradable and renewable properties. The probability of natural fibers such as kenaf, sisal, pineapple leaf, banana jute to produce polymer composites was studied (Faruk et al., 2012). Coconut coir is an inexpensive agricultural product that can be obtained in al large volume from the local community. It is a cheap eco-friendly fiber that is also less expensive than jute and sisal (Geethamma et al., 1998). The utilization of coconut coir as reinforcing fillers in polymer composites becomes more desirable due to their high strength and modulus properties (Macedo et al., 2010; Monteiro et al., 2008). Studies on powdered coconut coir as the filler has been appeared in the literature (Kaewduang et al., 2015; Sarki et al., 2011). This work aims to investigate the possibility of Coconut coir powders (CCP) of different particle sizes in using as reinforcement filler in the NR matrix. The effect of filler content on the properties of CCP/NR composites was investigated.

[1] Thailand Institute of Scientific and Technological Research, KhongLuang, Pathum Thani, 12120, Thailand
[*] Corresponding author: Email:siriporn@tistr.or.th

Materials and Methods

Preparation of Coconut coir powders

The coconut coir was collected from the shell of the matured coconut and was broken into small pieces. The coconut coir was oven-dried at 100 °C overnight for removing moisture. After drying, a portion of the coconut coir powders (CCP) was milled into fine particles by the blender machine and fed into a vibrating sieving machine using 300 um mesh which was called Fine CCP (F-CCP). A second portion, CCP were sieved through the previous mesh size without milling which was called Coarse-CCP (C-CCP). Their powder sizes were measured by an optical microscope and were used as the filler in NR composites. The average powder sizes of F-CCP and C-CCP were about 39 um and 101 um, respectively. And the morphology is shown in Figure 1.

Preparation of the composites

The formulation of the mixes was given in Table 1. The natural rubber used for the study was crepe rubber grade obtained from the local rubber companies. Coconut coir powders (CCP) were used as the filler. The composite compounds with different CCP loading were mixed using an internal mixer. The Sulphur and TMTD acted as a vulcanizing agent and were added during the milling step using a two-roll milling machine. The sheeted rubber compounds were kept for maturation at room temperature for 24 h until the mixture was hardened. After that, the rubber composite compounds were vulcanized in the compression-molding under 1 min preheating at 150 °C and compressed under a pressure of 75 kg/cm^2 (mold dimension: 160 x 160 x 2 mm^3).

Characterization

Mechanical properties

For the stress-strain behavior of composite samples, the Shimadzu Testing Machine (AG-X Plus 10kN model) was used. The tensile properties of the composites were tested according to ASTM D412-1998, at a crosshead speed of 500 mm/min at room temperature. The Hardness test on Shore-A Durometer according to ASTM D2240 was conducted using Bareiss Digi test II hardness tester. The specimen should be at least 6 mm thick and hardness reading was performed within three seconds during testing. Finally, the hardness was measured for five different positions and the average values were presented.

Physical properties

The swelling measurements of the composites were examined in the toluene. The specimen with a thickness of 2 mm was cut into a rectangular shape in the dimension of 25x25 mm. Then the composite samples were dried at 60°C for 24 h. The specimen was immersed in toluene for 48 h at 25°C. The swollen composite sample was taken out of the toluene and wiped with tissue paper to remove excess toluene. Then, the weight of the swollen samples was determined precisely. This data can be determined for the percentage of

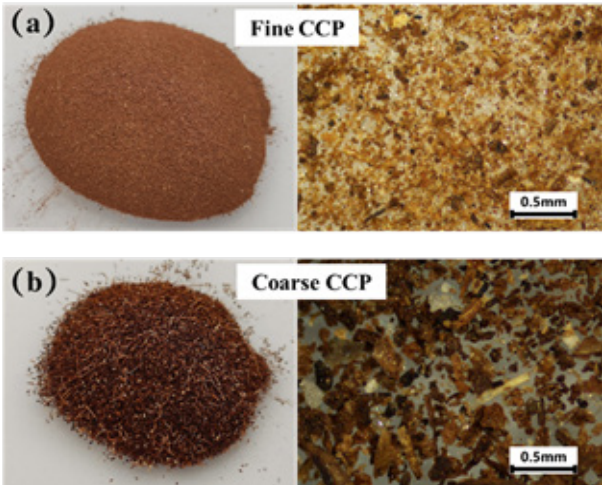

Figure 1. (a) CCP with milling by blender machine (F-CCP) and (b) CCP without milling (C-CCP) and both sieving thought 300 um sieve size

Table 1. Mixing formulations of composites

Ingredient	phra
Crepe rubber (NR)	100
ZnO	5
Stearic acid	2
Wingstay L	1
Ozone wax	1
Clay	100
White oil	1
CCPb	0, 25, 50, 75, 100
TMTDc	1
Sulfur	1.7

a Parts per hundred of rubber

b Coconut CoirPowders of both fine and coarse in particle sizes

c Tetramethylthiuram Disulfide

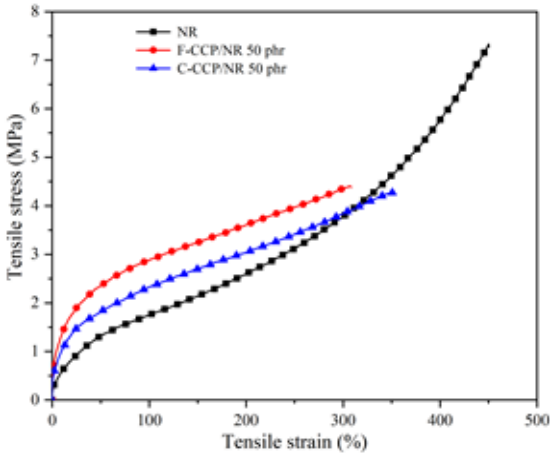

Figure 2. Stress-strain curves of NR, F-CCP/NR and C-CCP/NR composites with CCP content of 50 phr.

swelling and also rubber-filler interactions. The percentage of swelling can be calculated by;

$$\text{Swelling } (\%) = \frac{M - M_d}{M_d} \times 100 \qquad (2)$$

Where M and Md are the wet weight after removing the excess toluene and dry weight, respectively.

Results and discussion

Figure 2 shows the tensile stress-strain curves in CCP/NR composites with 50 phr of F-CCP and C-CCP. The NR sample without CCP loading exhibits a typical stress-strain behavior of vulcanized rubber showing the ultimate strain of around 440%. It is noted that all the CCP/NR composites have higher moduli than the NR sample. In the presence of 50 phr of C-CCP/NR composite, the ultimate strength and strain are reduced. Tensile strength was decreased by about 42% and strain at the break by 23%.

The CCP with the massive diameter causes deterioration in the properties due to the formation of voids at the CCP-matrix interface because of insufficient interfacial interaction (Parambath et al., 2019). Besides, the F-CCP/NR composite was observed that the tensile

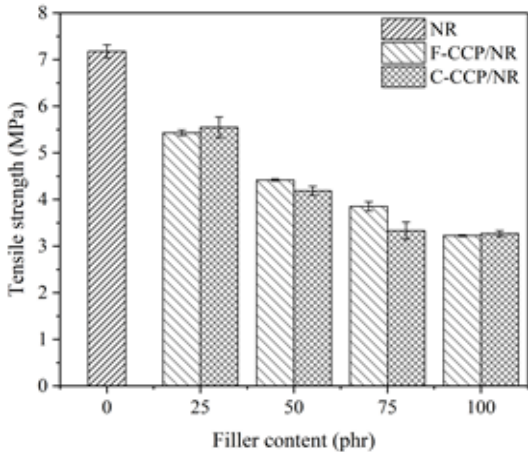

Figure 3. The effect of filler content on tensile strength of NR, F-CCP/NR and C-CCP/NR composites

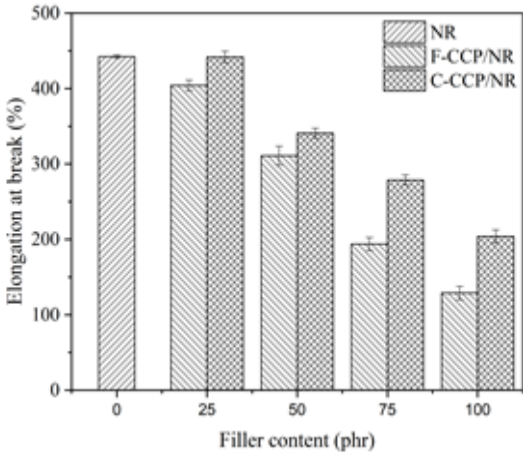

Figure 4. The effect of filler content on elongation at break of NR, F-CCP/NR and C-CCP/NR composites.

strength can be improved. Although the value of elongation at break decreased from 341% to 311%, however, the F-CCP/NR composites retain the elastic properties of the pure NR

The effect of filler loading with different CCP sizes on tensile strength of CCP/NR composites is shown in Figure 3. As observed, the increase of CCP contents affected in the weaken tensile strength when compared with the NR compound. For the CCP/NR composites, the increase of CCP content inducing tensile strength decreased. It is found that the maximum value of tensile strength at 25 phr of filler content. This result implies that the CCP/NR composite at 25 phr uniform the dispersion of filler in NR compounds and might be the effect of better interfacial adhesion due to a large interfacial area of contact contributes to a higher tensile strength (Balan et al., 2017; Herrera-Franco et al., 2004). When the filler contents are applied above 25 phr, the tensile strength decreased due to weak interaction and bonding between the filler and NR matrix are responsible for the decline of tensile strength. The other reason might be due to agglomeration. And, therefore, the filler – filler interaction of the CCP filler also increases (Balan et al., 2017). This is consistent with the study of Leha et al. which presents the effect of filler from 10 to 40 %. The filler content at 25% showed the highest tensile strength. For more addition of the filler, it presented a decrease in mechanical properties (Noor Leha et al., 2014). For the comparison of the tensile strength between F-CCP/NR and C-CCP/NR composites, it was found that the filler content at 25 and 100 phr, C-CCP/NR exhibited the value which closes to the value of F-CCP. However, the filler contents of 50 and 75 phr exhibit the tensile strength of F-CCP/NR higher value than C-CCP/NR. This is due to the effect of the high specific surface area of filler sizes on the NR matrix (Sareena et al., 2012).

Figure 4 shows the elongation at break of the CCP/NR composites is decreased with increasing filler content due to the addition of filler which reduces the mobility and increases the brittleness of the composites (Islam et al., 2017).

The lower elongation at high filler content might be due to the void portion is filled up according to the adding of filler content. Besides, the increase of CCP filler content in the NR compounds stiffens and also hardens the NR compounds. It will reduce resilience and toughness that leads to lower elongation. The toughness behavior is showed in Figure5. Comparing the elongation at break at the different size of CCP loading, it is observed that F-CCP/NR composites provide the higher elongation than those of C-CCP/NR composites. This result implies that it is due to better interaction between F-CCP and NR matrix (Parambath et al., 2019; Wongsorat et al., 2014).

Figure 6. shows the effect of filler content on the modulus of elasticity of F-CCP/NR and C-CCP/NR composites. Fillers are known to enhance the modulus, exhibited that the modulus of the filler is higher than that of the NR matrix (0 phr) (Sareena et al., 2012). In

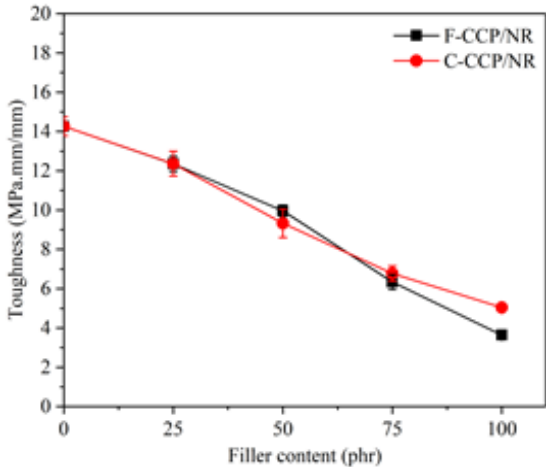

Figure 5. Effect of filler contenton the toughness of F-CCP/NR and C-CCP/NR composites.

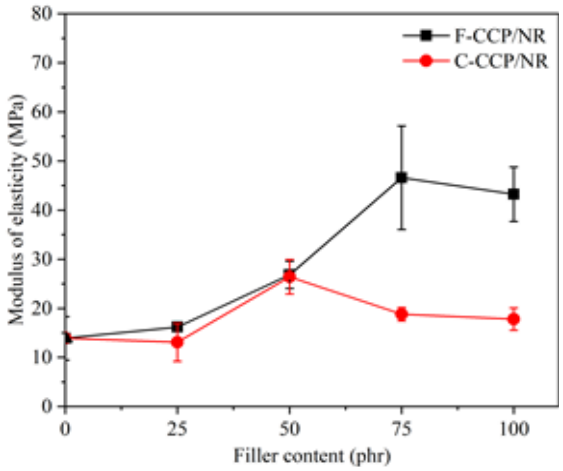

Figure 6. Effect of filler content on Modulus of elasticity of F-CCP/NR and C-CCP/NR composites.

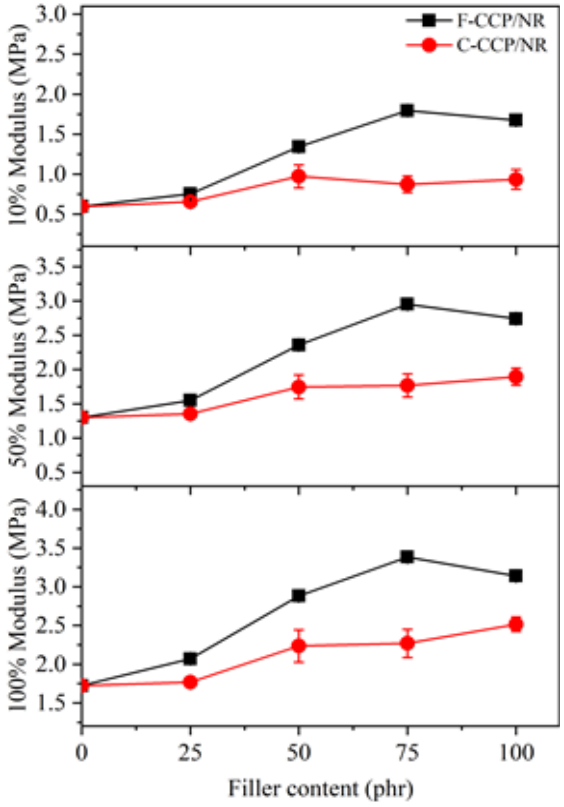

Figure 7. Moduli at (a) 10% strain, (b) 50%strain and (c) 100% strain of F-CCP and C-CCP filled NR composites

the case of F-CCP/NR, composites increase in the modulus with the filler content increasing almost linear up to 75 phr. While the modulus decreased when further increasing the filler content at 100 phr. For the C-CCP/NR composites, it exhibits an increase of modulus with the filler content up to 50 phr. Then an increasing filler content causes the modulus trend to decrease which is lower as compared with F-CCP/NR composites.

This result implies that modulus of F-CCP/NR composites improved due to the homogeneous distribution and their effective interaction with the matrix restain the molecular movement (Parambath et al., 2019). The agglomeration of filler at a higher loading does not act a disturbing effect on the modulus due to it is measured at low stains which the stress concentration is not enough for initiation of crack.

The effect of filler content on the reinforcing efficiency of F-CCP and C-CCP, moduli at 10%, 50%, and 100% strains of the composites are observed in Figure 6. This variation is a measure of the stiffness of compos-

ites. It can be shown that 10%, 50%, and 100% strains increase slightly with increasing filler content. This reveals that the filler powder acts like rigid particulates since it has a higher modulus than the NR matrix (Sareena et al., 2012). The moduli at 10%, 50% and 100% strains of the composites containing F-CCP were higher than those containing C-CCP. This indicates that the smaller sized filler in F-CCP/NR composites performed the higher modulus values than those of larger sized filler in C-CCP/NR composites.

Figure 8. shows the hardness of CCP/NR composites with different sizes and filler loading of CCP. Hardness increases with the increase in filler content. The hardness of F-CCP/NR composites exhibits higher values than C-CCP filled composites. Hardness is a measure of the resistance to deformation. The incorporation of fillers into an NR matrix reduces the elasticity of rubber. All fillers used are non-deformable solids and the addition of more rigid particles leads to increased rigidity and stiffness of the material.

The CCP/NR composites with different sizes of filler content characterized to examine swelling in toluene at room temperature for 48 h are presented in Figure 9. The highest swelling value is NR composite at 197% while the tendency swelling decreases with increasing of the filler loading in the NR composites. This implies that the filler loading in NR blends that restrict the molecular movement of the rubber.

This then made it more difficult for the toluene to penetrate through the rubber, thus, decreasing the swelling percentage. However, the swelling percentage decreased up to 50 phr in solvent uptake (%) at equilibrium swelling of CCP filled NR can be additionally described in the increase in contact surface area between polymer and filler.

At lower loading, the dominating effect is polymer-filler networks, whereas, at higher loading, the filler-filler networks will govern in the composites (Swapna et al., 2016). The result was related to the increase in tensile modulus, hardness, and also tensile strength for CCP filled NR composite.

Conclusion

In summary, this report presented the effect of particle sizes of fine and coarse coconut coir powders on the mechanical properties of NR and CCP/NR composites. All CCP/NR composites were prepared with 25, 50, 75, and 100 phr of CCP filler content. The increase in CCP content has decreased the tensile strength, elongation at break and toughness, whereas increasing the modulus of elasticity of CCP/NR composites. The result reveals that the CCP/NR composite of 25 phr filler loading exhibits better mechanical properties. F-CCP filler exhibits better mechanical properties and hardness as compared to C-CCP filler. The swelling values of CCP/NR composites in the toluene solution trend to decrease

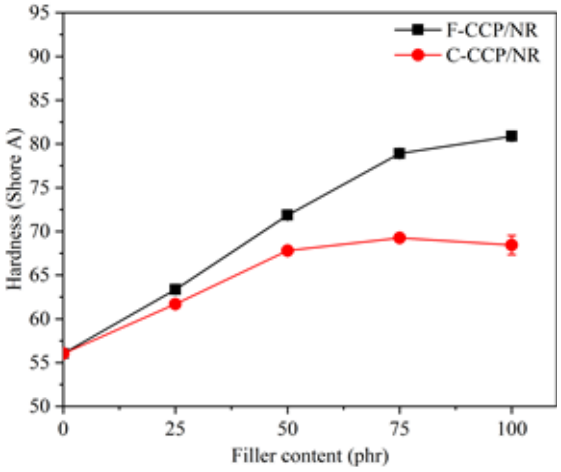

Figure 8. Variation of hardness with filler content for CCP/NR composites

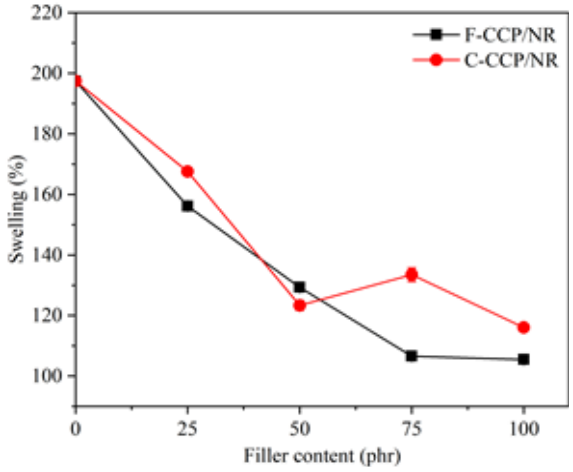

Figure 9. The effect of CCP loading on the swelling percentage of NR composites

with increasing filler loading in the NR composites. These results indicate that CCP/NR composites can be developed and apply for rubber mat.

Acknowledgments

The authors are grateful to The Expert Centre of Innovative Materials, Thailand Institute of Scientific and Technological Research (TISTR).

References

Balan, A. K., Mottakkunnu Parambil, S., Vakyath, S., Thulissery Velayudhan, J., Naduparambath, S., & Etathil, P. (2017). Coconut shell powder reinforced thermoplastic polyurethane/natural rubber blend-composites: effect of silane coupling agents on the mechanical and thermal properties of the composites. Journal of Materials Science, 52(11), 6712-6725. doi:10.1007/s10853-017-0907-y

Faruk, O., Bledzki, A. K., Fink, H.-P., & Sain, M. (2012). Biocomposites reinforced with natural fibers: 2000–2010. Progress in Polymer Science, 37(11), 1552-1596. doi:https://doi.org/10.1016/j.progpolymsci.2012.04.003

Geethamma, V. G., Thomas Mathew, K., Lakshminarayanan, R., & Thomas, S. (1998). Composite of short coir fibres and natural rubber: effect of chemical modification, loading and orientation of fibre. Polymer, 39(6), 1483-1491. doi:https://doi.org/10.1016/S0032-3861(97)00422-9

Herrera-Franco, P. J., & Valadez-González, A. (2004). Mechanical properties of continuous natural fibre-reinforced polymer composites. Composites Part A: Applied Science and Manufacturing, 35(3), 339-345. doi:https://doi.org/10.1016/j.compositesa.2003.09.012

Islam, M., Das, S., Saha, J., Paul, D., Islam, M., Rahman, M., & Khan, M. (2017). Effect of Coconut Shell Powder as Filler on the Mechanical Properties of Coir-polyester Composites. Chemical and Materials Engineering, 5, 75-82. doi:10.13189/cme.2017.050401

Ismail, H., Edyham, M. R., & Wirjosentono, B. (2002). Bamboo fibre filled natural rubber composites: the effects of filler loading and bonding agent. Polymer Testing, 21(2), 139-144. doi:https://doi.org/10.1016/S0142-9418(01)00060-5

Kaewduang, M., Chaichana, E., Jongsomjit, B., & Jaturapiree, A. (2015). Use of coir-filled LLDPE as a reinforcement for natural rubber composite. Paper presented at the Key Engineering Materials.

Luz, S. M., Gonçalves, A. R., & Del'Arco, A. P. (2007). Mechanical behavior and microstructural analysis of sugarcane bagasse fibers reinforced polypropylene composites. Composites Part A: Applied Science and Manufacturing, 38(6), 1455-1461. doi:https://doi.org/10.1016/j.compositesa.2007.01.014

Macedo, J. d. S., Costa, M. F., Tavares, M. I. B., & Thiré, R. M. S. M. (2010). Preparation and characterization of composites based on polyhydroxybutyrate and waste powder from coconut fibers processing. Polymer Engineering & Science, 50(7), 1466-1475. doi:10.1002/pen.21669

Monteiro, S. N., Terrones, L. A. H., & D'Almeida, J. R. M. (2008). Mechanical performance of coir fiber/polyester composites. Polymer Testing, 27(5), 591-595. doi:10.1016/j.polymertesting.2008.03.003

Noor Leha, A. R., & Nordin, N. A. (2014). Effect of Filler Compositions on the Mechanical Properties of Bamboo Filled Polyester Composite. Advanced Materials Research, 879, 90-95. doi:10.4028/www.scientific.net/AMR.879.90

Panthapulakkal, S., Zereshkian, A., & Sain, M. (2006). Preparation and characterization of wheat straw fibers for reinforcing application in injection molded thermoplastic composites. Bioresource Technology, 97(2), 265-272. doi:https://doi.org/10.1016/j.biortech.2005.02.043

Parambath Kanoth, B., Thomas, T., Joseph, J. M., & Narayanankutty, S. K. (2019). Restructuring of coir to microfibers for enhanced reinforcement in natural rubber. Polymer Composites, 40(1), 414-423. doi:10.1002/pc.24667

Sareena, C., Ramesan, M. T., & Purushothaman, E. (2012). Utilization of coconut shell powder as a novel filler in natural rubber. Journal of Reinforced Plastics and Composites, 31, 533-547. doi:10.1177/0731684412439116

Sarki, J., Hassan, S. B., Aigbodion, V. S., & Oghenevweta, J. E. (2011). Potential of using coconut shell particle fillers in eco-composite materials. Journal of Alloys and Compounds, 509(5), 2381-2385. doi:https://doi.org/10.1016/j.jallcom.2010.11.025

Swapna, V. P., Stephen, R., Greeshma, T., Sharan Dev, C., & Sreekala, M. S. (2016). Mechanical and swelling behavior of green nanocomposites of natural rubber latex and tubular shaped halloysite nano clay. Polymer Composites, 37(2), 602-611. doi:10.1002/pc.23217

Wongsorat, W., Suppakarn, N., & Jarukumjorn, K. (2014). Effects of compatibilizer type and fiber loading on mechanical properties and cure characteristics of sisal fiber/natural rubber composites. Journal of Composite Materials, 48(19), 2401-2411. doi:10.1177/0021998313498790

Investigation of Physical and Mechanical Properties of Colored TiO_2 Thin Films deposited by RF Magnetron Sputtering

Busarin Noikaew[1,*], Laksana Wangmooklang[1]
and Siriporn Larpkiattaworn[1]

Received May 28, 2020; Revised, June 10, 2020; Accepted June 29 2020

Abstract

The colored titanium dioxide (TiO_2) thin films were prepared by RF magnetron sputtering technique using purity TiO_2 target. In this study, the deposition time for sputtering process was varied from 60, 75, 90, 105 and 120 minutes by using the fixed appropriate sputtering power at 100 W. The working pressure of argon gas was kept constant at 6.0x10-1 Pa. As a consequence, TiO_2 thin films were deposited on both glass and stainless steel substrates for color's film observation. To study the physical and mechanical properties of colored TiO_2 thin films, optical transmission, surface morphology and structure were investigated by using UV-Vis Spectrophotometer, FESEM and XRD, thin film thickness and adhesion were measured by calotester and micro scratch tester, respectively. It was found that the colored TiO_2 thin films were clearly observed on both substrates. The optical transmission for TiO_2 films showed highly transmission in the visible regions and surface morphologies showed nano-scale grain size and smooth surface. The structure of all TiO_2 thin films exhibited amorphous structure. For these results, thicknesses of colored TiO_2 thin films are approximately 70 nm to 150 nm. In addition, the adhesion of colored films performed a good adhesion by increasing deposition time.

Keyword: TiO_2 thin film, Colored thin film, RF magnetron sputtering

Introduction

Titanium dioxide (TiO_2) thin film is attractive and utilizing material for many applications because of their interesting physical, chemical, optical and electrical properties. Many applications of TiO_2 thin film are extensively such as photovoltaic materials (Timoumi, Alamri and Alamri, 2018), photocatalytic properties (Zahedi et al., 2015), gas sensor (Salman, Shihab, and Elttayef, 2019), hydrophilic and hydrophobic properties (Xiong et al., 2015; Bharti, Kumar and Kumar, 2016; Gao et al., 2015). The physical and chemical techniques have been applied to fabricate the TiO_2 thin films such as spray (Momeni et al., 2015), sol-gel (Jiang, et al., 2019; Meher and Balakrishnan, 2014), pulse laser (Zhang et al., 2015; Ishii et al., 2015), chemical vapor deposition (Astinchap and Laelabadi, 2019) and sputtering (Guillén and Herrero, 2017; Nezar et al., 2017). However, for enhancing thin film uniformity and adhesion on a substrate, the magnetron sputtering is a more favorable technique for many types of coating materials such as oxides, nitrides, carbides, fluorides and arsenides than that of the wet process. One of the most attractive thin films is the variation of colors, especially gold-like color. Regularly, many composite thin films including metal oxides as well as nitrides such as TiN, ZnO, ZrN, AlTiN and TiO_2 have their specific colors for decorative and hard coatings (Neugebohrn et al., 2019; Niyomsoan et al., 2002; Panjan et al., 2014). In this work, the colored TiO_2 films were fabricated by radio frequency (RF) magnetron sputtering on glass and stainless steel (SS) substrates for color change monitoring in order to investigate the adhesion of colored thin films. The deposition time were varied from 60 - 120 minutes with constant RF power and argon (Ar) gas pressure during deposition process.

[1] Expert Centre of Innovative Materials, Thailand Institute of Scientific and Technological Research (TISTR)
35, Mu. 3, Khlong Ha, Khlong Luang Pathum Thani, 12120, Thailand
Tel: +662 577 9431 Fax: +662 577 9426, MP: +668 6792 9009,
* Corresponding author. Email: busarin@tistr.or.th

For observing the adhesion of thin film, one of the outstanding mechanical instruments is the scratch tester which causes surface failure to indicate the adhesion and scratch resistance of the films (Mercier et al., 2017; Zivica et al., 2012). The optical properties of colored films were characterized by UV-Vis Spectrophotometer, the morphologies were characterized by Field Emission Scanning Electron Microscope (FESEM). Thin film structures were analyzed by X-ray diffractometer (XRD), For mechanical testing, the thicknesses of TiO_2 films were measured by calotest technique and thin film adhesion and scratch resistance were observed by micro scratch tester.

Experiment

1. Thin film fabrication

The various colored TiO_2 thin films were fabricated by RF magnetron sputtering technique using 99.95% purity TiO_2 ceramic target with thickness and diameter of 6 mm and 50.8 mm, respectively. TiO_2 films were deposited onto 1 mm thick of slide glass (2.54 cm x 7.62 cm) and 2 mm thick of stainless steel (3 cm x 3 cm) substrates. Prior to deposition, glass and stainless steel substrates were cleaned ultrasonically in acetone, methanol and deionized water for 15 minutes and then dried before loading into the deposition chamber. The distance between the target and substrate holder was fixed at 10 cm. Base pressure in the chamber was approximately 2.0×10^{-4} Pa at starting the sputtering process. Then, argon sputtering gas was feed into the chamber with the controlled working pressure at 6.0×10^{-1} Pa and RF power were kept constant and 100 W. In this study, TiO_2 thin film was deposited at room temperature and the substrate holder was continuously rotated by varying the deposition time from 60, 75, 90, 105 and 120 minutes. For thin film characterization, the optical transmission, surface morphology, structure, thickness and the adhesion were investigated.

2. Thin film characterization

Optical properties of the colored TiO_2 thin films deposited on glass substrate were analyzed by UV-Vis Spectrophotometer (UV-1700, SHIMADZU). Surface morphologies of the colored TiO_2 thin films were observed by Field Emission Scanning Electron Microscope operated at 5 kV (FESEM, JEOL JSM-6340F). The structures were characterized by X-ray diffractometer (XRD, Rigaku SmartLab). Besides, thicknesses of the TiO_2 thin films were characterized by calotester (Calotest compact CATc, Anton Paar). In addition, the adhesion and scratch resistance of the colored TiO_2 films were investigated by using Micro Scratch Tester with Rockwell diamond stylus indenter (MST3, Anton Paar).

Results and discussion

TiO_2 thin films grown on glass and stainless steel substrates can be observed with the observers' naked eyes in Figure 1. When the deposition time increased from 60-120 minutes, the colors were varied and adhered on both glass and stainless steel substrates. TiO_2 thin films grown on glass substrate, the colored were slightly changed from purple, blue, green, orange and pink. In case of stainless steel substrates, the colored were quite different from the colors on glass substrate as blue, green, gold, rose gold and pink because of the reflection of substrate material. It can be obviously seen that the different substrates can lead to slightly different colored films.

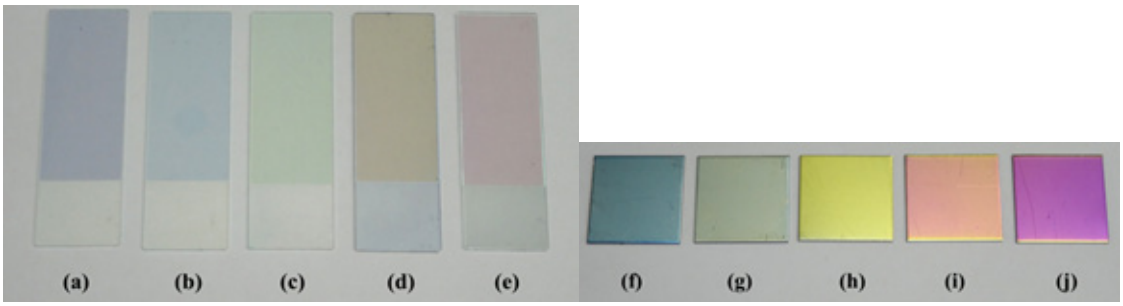

Figure 1. The colored TiO_2 thin films grown on glass and stainless steel substrates by increasing deposition time, (a,f) 60 minutes, (b,g) 75 minutes, (c,h) 90 minutes, (d,i) 105 minutes and (e,j) 120 minutes.

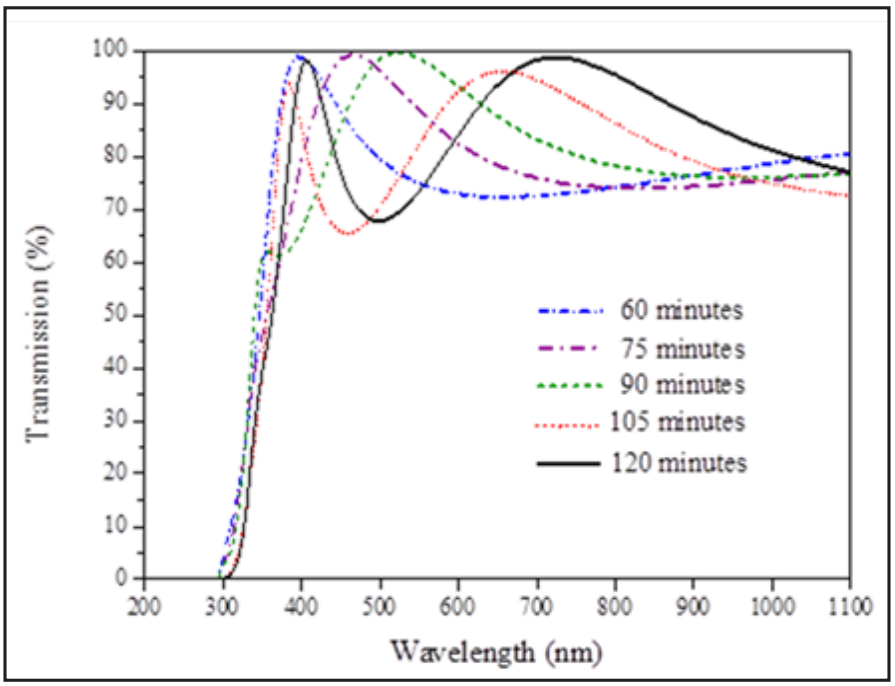

Figure 2. The optical transmission of TiO_2 thin films by varying deposition time from 60-120 minutes.

1. Optical transmissions

Optical transmission spectra of different deposition time of TiO_2 thin films grown on glass substrates was measured as the function of wavelengths ranging between 300 nm and 1100 nm by UV-Vis Spectrophotometer as seen in Figure 2. In order to increase deposition time from 60-120 minutes with constant sputtering power at 100 W, TiO_2 thin films obtained highly transmission around 70-98% with a sharply absorption edge around 300-320 nm. The transparency levels of the films for 105 and 120 minutes were slightly lower and the absorption edges were slightly higher. It can be indicated that the increase of deposition time can cause increasing thin film thickness which related with band gap energy. In addition, all TiO_2 thin films had high transmission in the visible range (400-700 nm) which could be easily observed by naked eyes. As a result, the interference layer of thin film and the substrate is also depended on thin film thickness.

2. Surface morphologies

The results of different deposition time on surface morphologies of the TiO_2 thin films grown on glass substrate were observed by FESEM as shown in Figure 3. Surface morphologies of all TiO_2 films were comparatively nano-scale particle size and smooth surface. For the deposition time at 60 minute, the surface morphologies were rather smaller and denser particles than those of other conditions. In case of increasing deposition time, the morphologies had rather bigger and rougher than the less time deposition. It can be suggested that the sputtered particles had more time to arrange themselves and accumulate on the substrates.

3. Thin film structures

The structure of TiO_2 thin films by varying deposition time were characterized by x-ray diffractometer with gracing incident at 1o between incident x-ray and substrate. The x-ray diffraction patterns of TiO_2 thin film by increasing deposition time can be seen in Figure 4. All TiO_2 thin films compared with a bare glass substrate showed amorphous structure even though the deposition time was increased. These results could be explained that TiO_2 thin films deposited at room temperature have no activated energy by thermal treatment from the substrate to rearrange and enhance the crystalline structure.

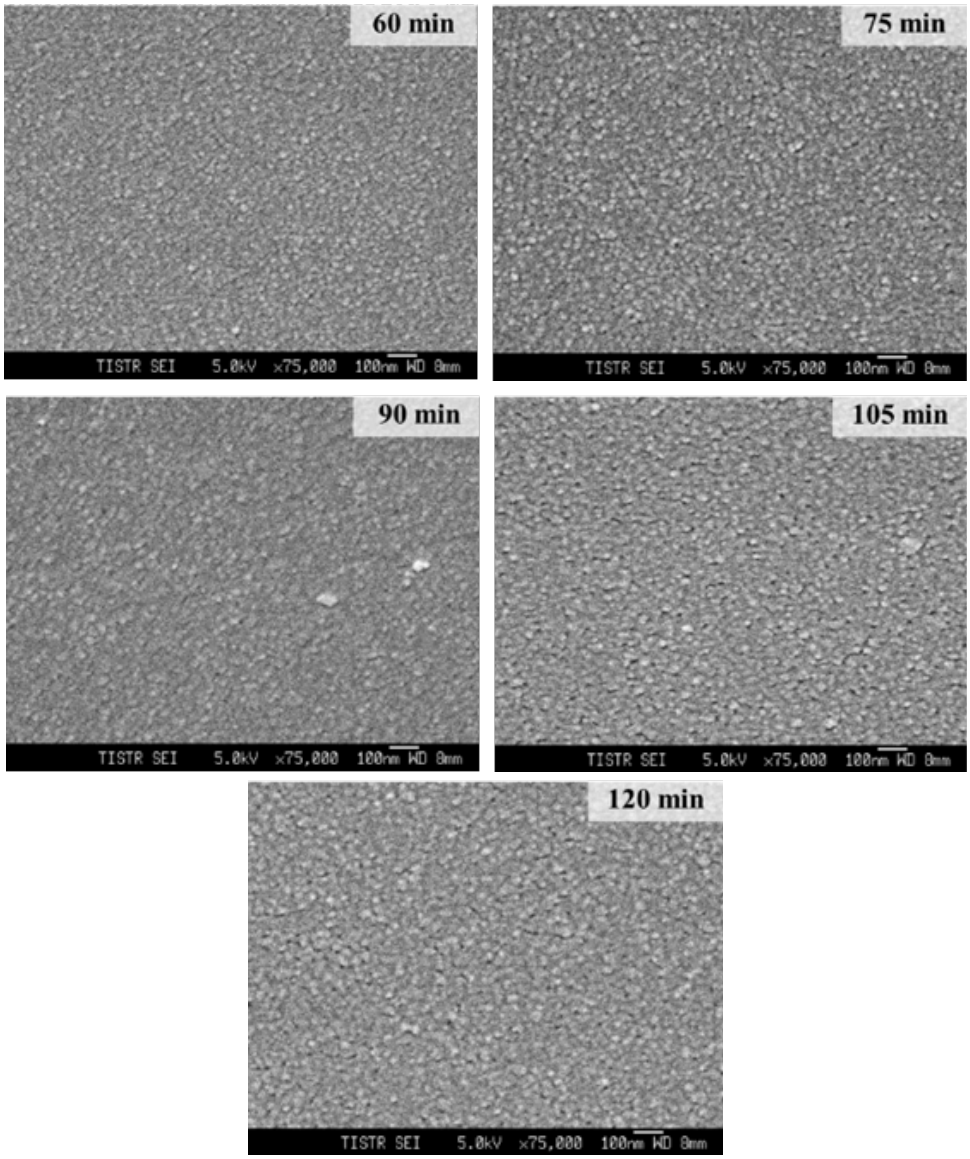

Figure 3. Surface morphologies of TiO_2 thin films by varying deposition time from 60-120 minutes.

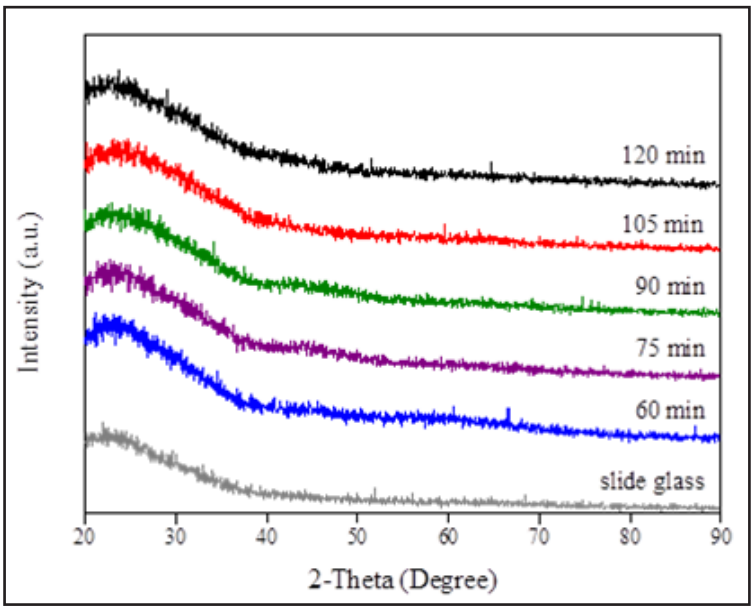

Figure 4. Structure of TiO_2 thin films by varying deposition time from 60-120 minutes.

4. Thin film thicknesses

The thickness of various colored TiO_2 thin films grown on glass substrate were measured by calotester. In this method, the sample was fixed at the stage and a rotating steel ball with a 20 mm diameter rotated on a thin film surface. Thus, the difference between abrasive layer of TiO_2 thin film and glass substrate is the thickness of the film. For various colored TiO_2 thin film, the thicknesses were increased by increasing the deposition time. When the deposition time increased from 60 – 120 minutes, the thicknesses of TiO_2 thin films are absolutely increased from 70.1 – 151.2 nm. TiO_2 thin film gained the average deposition rate around 1.22 nm/min (The deposition rate was defined by a ratio between thickness to deposition time) with the standard deviation of 0.03. Thicknesses and deposition rates of TiO_2 thin films by varying deposition time from 60-120 minutes can be seen in Table 1 and Figure 5.

5. Thin film adhesions

The adhesion of the colored TiO_2 thin films deposited on stainless steel was measured by micro scratch tester with a normal force from 0.01 N to 2.00 N. However, thin film coating quality is related to the adhesion characteristics between thin film and substrate. The surface failure behavior of each sample was observed under a microscope scratching with a progressive load along the scratch distance of 2 mm. Three different types of critical load (Lc) were indicated along the scratch trace; a start of the scratch (Lc1), delamination (Lc2) and complete delamination (Lc3) as shown in Table 2. Figure 6 shows the optical photographs of the scratch trace of increasing deposition from 60-120 minutes. The scratch testing results of TiO_2 thin films deposited from 60-120 minutes had the complete delamination at critical load of approximately 1.09 N - 1.80 N, respectively. As a result, colored TiO_2 thin films per-

Table 1. Thicknesses and deposition rates of TiO_2 thin films by varying deposition time from 60-120 minutes.

Deposition time (minutes)	Deposition rate (nm/min)	Thickness (nm)
60	1.17	70.1
75	1.21	91.0
90	1.24	111.3
105	1.20	126.0
120	1.26	151.2

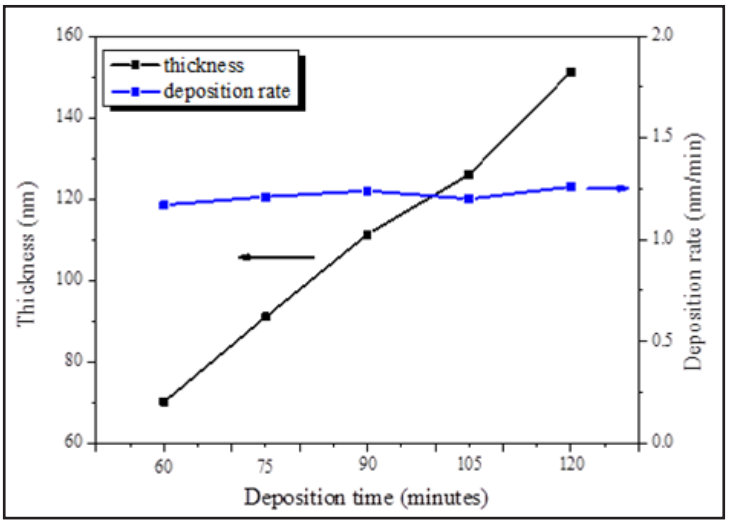

Figure 5. Thicknesses and deposition rates of TiO_2 thin films by varying deposition time from 60-120 minutes.

formed good adhesion on the substrate because of preparing by PVD technique even though the structures of the film had amorphous structure. Moreover, the maximum deposition time as well as maximum thickness exhibits the longer distance of delamination than those of thinner thickness.

Conclusions

The physical and mechanical properties of colored TiO_2 thin films prepared by RF magnetron sputtering technique were studied on both physical and mechanical properties such as the transmission, morphology, structure, thickness and the adhesion of the films. The thicknesses of the films were increased from 70.1-151 nm with increasing deposition time at 60-120 minutes with approximately constant deposition rate. Then, the colors of thin film can also be change by the thickness and the interference of light on substrates. The colored TiO_2 thin films have high transmission around 70-98% at the visible range region. Then, the surface morphologies exhibit smooth surface with nano-scale particle size and then the structure of colored TiO_2 thin films show amorphous structure due to no thermal treatment during thin film deposition. Moreover, scratch testing results show good adhesion between various TiO_2 thin films and the substrate.

Table 2. The critical load of scratch testing by varying deposition time from 60-120 minutes.

Deposition time (minutes)	Lc1 (N)	Lc2 (N)	Lc3 (N)
60	0.20	0.50	1.09
75	0.21	0.64	1.15
90	0.21	0.69	1.34
105	0.23	0.97	1.44
120	0.27	1.29	1.80

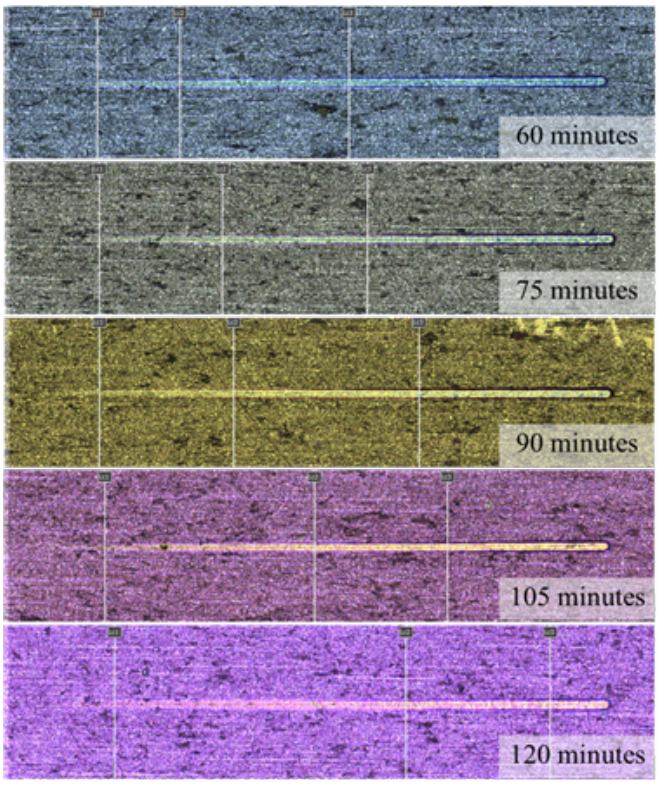

Figure 6. The scratch traces with critical loads of TiO_2 thin films by varying deposition time from 60-120 minutes.

Acknowledgements

The authors are sincerely grateful to the National Research Council of Thailand (NRCT) for financial support. The Expert Centre of Innovative Materials, Thailand Institute of Scientific and Technological Research (TISTR) is greatly acknowledged.

References

Astinchap, B. and Laelabadi, K. G. (2019). Effects of substrate temperature and precursor amount on optical properties and microstructure of CVD deposited amorphous TiO2 thin films. Journal of Physics and Chemistry of Solids, 129, 217-226.

Bharti, B., Kumar, S. and Kumar, R. (2016). Superhydrophilic TiO2 thin film by nanometer scale surface roughness and dangling bonds. Applied Surface Science, 364, 51-60.

Gao, Z., Zhai, X., Liu, F., Zhang, M., Zang, D. and Wang, C. (2015). Fabrication of TiO2/EP superhydrophobic thin film on filter paper surface. Carbohydrate Polymers, 128, 24-31.

Guillén, C. and Herrero, J. (2017). TiO2 coatings obtained by reactive sputtering at room temperature: Physical properties as a function of the sputtering pressure and film thickness. Thin Solid Films, 636, 193–199.

Ishii, A., Nakamura, Y., Oikawa, I., Kamegawa, A. and Takamura, H. (2015). Low-temperature preparation of high-n TiO2 thin film on glass by pulsed laser deposition. Applied Surface Science, 347, 528–534.

Jiang, Y., Shi, K., Tang, H. and Wang, Y. (2019). Enhanced wettability and wear resistance on TiO2/PDA thin films prepared by sol-gel dip coating. Surface and Coatings Technology, 375, 334-340.

Meher, S.R. and Balakrishnan, L. (2014). Sol–gel derived nanocrystalline TiO2 thin films: A promising candidate for self-cleaning smart window applications. Materials Science in Semiconductor Processing, 26, 251–258.

Mercier, D., Mandrillon, V., Parry, G., Verdier, M., Estevez, R., Bréchet, Y. and Maindron, T. (2017). Investigation of the fracture of very thin amorphous alumina film during spherical nanoindentation. Thin Solid Films, 638, 34–47.

Momeni, M. Golestani-Fard, F., Saghafian, H., Barati, N. and Khanahmadi, A. (2015). Development of visible light activated TiO2 thin films on stainless steel via sol spraying with emphasis on microstructural evolution and photocatalytic activity. Applied Surface Science, 357, part B, 1902-1910.

Neugebohrn, N., Gehrke, K., Brucke, K., Götz, M. and Vehse, M. (2019). Multifunctional metal oxide electrodes: Colour for thin film solar cells. Thin Solid Films, 685, 131–135.

Nezar, S., Saoula, N., Sali, S., Faiz, M., Mekki, M., Laoufi, N. A. and Tabet, N. (2017). Properties of TiO2 thin films deposited by rf reactive magnetron sputtering on biased substrates. Applied Surface Science, 395, 172–179.

Niyomsoan, S., Grant, W., Olson, D. L. and Mishra, B. (2002). Variation of color in titanium and zirconium nitride decorative thin films. Thin Solid Films, 415, 187-194.

Panjan, M., Klanjšek Gunde, M., Panjan, P. and čekada, M. (2014). Designing the color of AlTiN hard coating through interference effect. Surface and Coatings Technology, 254, 65-72.

Salman, S. H., Shihab, A. A. and Elttayef, A. – HK. (2019). Design and construction of Nanostructure TiO2 thin film gas sensor prepared by R.F magnetron sputtering technique. Energy Procedia, 157, 283-289.

Timoumi, A., Alamri S. N. and Alamri, H. (2018). The development of TiO2-graphene oxide nano composite thin films for solar Cells. Results in Physics, 11, 46-51.

Xiong, Y., Lai, M., Li, J., Yong, H., Qian, H., Xu, C., Zhong, K. and Xiao, S. (2015). Facile synthesis of ultra-smooth and transparent TiO2 thin films with superhydrophilicity. Surface and Coatings technology, 265, 78-82.

Zahedi, F., Behpour, M., Ghoreish, S. M. and Khalilia, H. (2015). Photocatalytic degradation of paraquat herbicide in the presence TiO2 nanostructure thin films under visible and sun light irradiation using continuous flow photoreactor. Solar Energy, 120, 287–295.